Iranian Journal of Pharmaceutical Research (2021), 20 (1): 359-370
DOI: 10.22037/ijpr.2020.113052.14089
Received: January 2020
Accepted: July 2020

Original Article

Evaluation of Molecular and Cellular Alterations Induced by Neuropathic Pain in Rat Brain Glial cells

Mohsen Rezaei[a], Lida Karimian[b], Bizhan Shafaghi[b], Maryam Noubarani[c], Maryam Salecheh[d], Mohammad Shafi Dehghani[d], Mohammad Reza Eskandari[e, c*] and Jalal Pourahmad[b*]

[a]Department of Toxicology, Faculty of Medical Sciences, Tarbiat Modares University, Tehran, Iran. [b]Department of Pharmacology and Toxicology, Faculty of Pharmacy, Shahid Beheshti University of Medical Sciences, Tehran, Iran. [c]Department of Pharmacology and Toxicology, School of Pharmacy, Zanjan University of Medical Sciences, Zanjan, Iran. [d]Department of Pharmacology and Toxicology, School of Pharmacy, Jundishapur University of Medical Sciences, Ahvaz, Iran. [e]Zanjan Pharmaceutical Nanotechnology Research Center (ZPNRC), Zanjan University of Medical Sciences, Zanjan, Iran.

Abstract

Neuropathic pain originates from illness or damage of the nervous system and affects the somatosensory system. Recently, many efforts have been made to illuminate the influences of neuropathic pain in different parts of central nervous system (CNS). However, the toxic consequences of neuropathic pain in glial cells, which involve in the control of pain is poorly understood. Therefore, the present study aimed to assess the molecular and cellular effects of neuropathic pain in the glial cells of rat brain. Induction of neuropathic pain in rats was associated with oxidative stress as evident by elevated reactive oxygen species (ROS) formation as well as reversible glutathione (GSH) depletion in the glial cells. Moreover, neuropathic pain caused mitochondrial membrane potential collapse ($\Delta\Psi m\%$), lysosomal membrane rapture, and proteolysis, probably due to ROS-induced MPT pore opening. These toxic events could cause cytochrome c release from intermembrane space into the cytosole and trigger caspase activation pathway. Our finding confirmed that the activity of caspase-3 was significantly increased in the glial cells as a core component of the apoptotic machinery. In conclusion, the neuropathic pain induces ROS generation as the major cause of GSH depletion along with mutual mitochondrial/lysosomal potentiation (cross-talk) of oxidative stress in the glial cells. Subsequently, this toxic cross-talk can induce proteolysis and trigger apoptosis by caspase-3 activation in the glial cells of rat brain.

Keywords: Glial cell; Oxidative stress; Lysosome; Cell death; Proteolysis; Caspase-3.

Introduction

It is believed that pain is a warning system that plays major role in the human body, including warning about damaged tissues, taking away from the source of the damage, and ultimately reduced activity to accelerate the healing process (1-3). Pain can be psychogenic or somatogenic, in which the somatogenic pain comprises nociceptive and neuropathic pain. Somatic or visceral nerve fibers activation by harmful agents create the nociceptive pain, whereas dysfunction of the central or peripheral nervous system leads to neuropathic pain (4, 5). The neuropathic

* Corresponding authors:
E-mail: j.pourahmadjaktaji@utoronto.ca;
eskandarimr@zums.ac.ir

pain, which can be due to peripheral or central neuropathy, is common and seriously disables millions of people around the world. The peripheral neuropathy arises from trauma, muscle atrophy along the nerve, connective tissue disease, malignancies, and diabetes, while central neuropathy occurs due to overlap disks, sub arachnoids inflammation, *etc.* (6, 7).

Damage to the nervous system has many molecular and cellular consequences and causes transformation and regeneration of neurons in anatomically different parts of nervous system (8-10). Glial cells or simply glia is known as a potent modulator of pain sensation and considered as a tool, which provides a new target for discovery of more effective drugs for pain alleviation (11). In the recent years, glial cells were found to modify neuronal function in the biological and pathological conditions (12). Glial deactivation in the brain or the spinal cord reduced pain induced by factors, such as inflammation of the peripheral nerves, spinal nerve transection, and the inflammation of the skin (13-15). On the other hand, glial cells apparently have no effect on the acute pain responses and specifically involve in pathological pains (16-18).

Chronic neuropathic pain and hyperalgesia possibly provoke neuronal cell death in the dorsal horn of the spinal cord, thus enlightening the processes involved in neuronal damage might identify the mechanisms of chronic neuropathic pain (12, 19). However, most of the consequences of neuropathic pain in glial cells have not yet been completely understood. Thus, the present study was designed to evaluate the molecular and cellular alterations induced by neuropathic pain in rat brain glial cells. Moreover, the role of cellular death in these toxic events was investigated.

Experimental

Chemicals

Bovine serum albumin (BSA), collagenase (from Clostridium histolyticum), N-Ethylmaleimide (NEM), O-phthalaldehyde (OPT), and rhodamine 123 were purchased from Sigma-Al- drich Co. (Taufkirchen, Germany). All other chemicals were of the highest commercial grade available.

Animals

Male Sprague-Dawley rats weighing 180 to 200 g were housed in ventilated plastic cages over PWI 8-16 hardwood bedding. There were 12 air changes per h, 12 h light photoperiods, an environmental temperature of 21–23 °C, and a relative humidity of 50–60 %. The animals were fed a standard normal chow diet and given tap water ad libitum. Principles of laboratory animal care (NIH publication No. 85-23, revised 1985) were followed. All experiments were conducted according to the ethical standards and protocols approved by the Committee of Animal Experimentation of Shahid Beheshti University of Medical Sciences, Tehran, Iran (protocol approval number: 88/01/94/6555).

Induction of neuropathic pain

Under 10% chloral hydrate (3 mL/kg) anesthesia the skin on the lateral surface of the thigh was incised and a section made directly through the biceps femoris muscle exposing the sciatic nerve and its three terminal branches: the sural, common peroneal, and tibial nerves. The Spared Nerve Injury (SNI) procedure comprised an axotomy and ligation of the tibial and common peroneal nerves leaving the sural nerve intact. The common peroneal and the tibial nerves were tight-ligated with 5.0 silk and sectioned distal to the ligation, removing 2–4 mm of the distal nerve stump. Great care was taken to avoid any contact with or stretching of the intact sural nerve. Muscle and skin were closed in two layers. Crush controls (spared nerve crush group) were performed as above, except that the tibial and common peroneal nerves were crushed for 30 s by a pair of small arterial forceps with smooth protective pads over the blades. At the end of this procedure the nerves were completely flattened and transparent. Sham controls involved exposure of the sciatic nerve and its branches without any lesion (20).

Mechanical hyperalgesia

After SNI pain evaluation was performed to confirm the occurrence of allodynia or hyperalgesia in the rat model. With the animals on the elevated grid, a pinprick test was performed using a safety pin. The lateral part of the plantar surface of the paw was briefly

stimulated at an intensity sufficient to indent but not penetrate the skin (pin-prick test). The duration of paw withdrawal was recorded, with an arbitrary minimal time of 0.5 s (for the brief normal response) and a maximal cut-off of l0 s (21).

Our results confirmed the induction of hyperalgesia in the neuropathic pain rat model. The withdrawal duration (in seconds) after a pin prick stimulus to the lateral plantar surface of the paw increased significantly after SNI. The SNI group's elevated response (pin-prick hyperalgesia) persisted for the entire time the animals were monitored (2 weeks) (Data not shown).

Study design

The rats were randomly divided into three different groups of 24 rats each. Group 1 (Control) animals fed with a standard diet and served as a normal control without surgery. Group 2 (Sham) rats that the SNI surgery was performed and was exposed to the sciatic nerve and its three terminal branches but without ligated and cutoff the common peroneal and tibial nerves. Group 3 (Case or neuropathic pain model) rats that the SNI surgery was performed along with ligated and cutoff the common peroneal and tibial nerves.

Glial cells isolation

On the second, 6^{th}, 10^{th}, and 14^{th} days after the surgery, the glia cells were taken. For this, brain was removed and placed in PBS buffer, hemispheres were separated and the bean-shaped hippocampi were isolated. Hippocampus was placed in dishes containing PBS, gently minced and pipetting up and down then incubated in a buffer contains trypsin-EDTA for 5 min at 37 °C. Then, it was smoothly shacked and again incubated for additional 5 min. Afterward, DMEM medium was added. The prepared suspension passed through the funnel (70 mesh, 25 micron) by the vacuum pump for elimination of neurons and oligodendrocytes. The cells were suspended at a density of 10^6 cells/mL in round bottomed flasks rotating in a water bath maintained at 37 °C in Krebs–Henseleit buffer (pH 7.4), supplemented with 12.5 mM HEPES under an atmosphere of 10% O_2, 85% N2, and 5% CO2. The cell suspensions were poured into round bottom flasks and were placed in a bioreactor for 15 min. Glia cells was placed in 1 mL of each in eppendorf tubes and was centrifuged for 1 min at 1000 rpm (22).

Glial cell identification

To confirm that a majority of isolated cells were glial cells, cells were analyzed for the expression of astrocyte marker glial fibrillary acidic protein (GFAP) through antibody staining. GFAP immunostained samples confirms that 90% of cells present are GFAP positive cells (Immunostaining data not shown).

Determination of reactive oxygen spices (ROS)

To measure the rate of glial cells ROS formation, non-fluorescent dichlorofluorescin diacetate (DCFH-DA) was used that hydrolyze to dichlorofluorescin (DCFH) (non-fluorescent) inside the cells. DCFH reacted with intracellular ROS and converted to the highly fluorescent dichlorofluorescein (DCF) that outflow the cell. For this purpose, 3 ml of cells were centrifuged for 1 min at 1000, then mixed with 3 mL of DCFH diacetate. The suspension was shaken gently and incubated for 10 min at 37 °C. The amount of ROS was measured according to fluorescence intensity by the fluorescence spectrometer (Excitation: 500 nm, Emission: 520 nm). The results were expressed as fluorescent intensity per 10^6 cells (23).

Determination of intracellular reduced glutathione (GSH)

The amounts of reduced and oxidized glutathione were assessed by the spectrofluorometric method with a few modifications (24). For the measurement of GSH, 1 mL of the cell suspension was centrifuged (1000 rpm, 1 min), and the supernatant was removed. Trichloroacetic acid (10%) was added to the cell pellet. After centrifugation (11000 rpm, 1 min), 4.5 mL of the incubation buffer (pH 8) was added to the supernatant (0.5 mL) then mixed with 100 µL of OPT (1 mg/mL). Incubation buffer (1.8 mL) was added to 100 µl of diluted supernatant in the previous step and incubated for 15 min at room temperature. The intensity was measured at Excitation: 350 nm and Emission: 420 nm.

Measurement of extracellular oxidized glutathione (GSSG)

1ml of the cell suspension centrifuged (1000 rpm, 1 min) and the supernatant was mixed with trichloroacetic acid 10%. After centrifugation (11000 rpm, min 1), 0.5 mL of the supernatant from the previous step mixed with NEM (0.04 M, 200 µM) for 30 min at room temperature. Measurement was similar to the GSH determination, except for incubation buffer that was replaced by NaOH (0.1 N) instead as diluents. The amount of GSH and GSSG was calculated by calibration curves (24).

Determination of glutathione precursors for compensation biosynthesis

After the incubation of glial cells with DMEM medium, the flasks were centrifuged (1000 rpm, 1 min). Incubation buffer (10 mL) was added to the cell pellet and the cell suspension again was transferred into the flask, then incubated with two glutathione precursors, methionine and betaine, for 3 h. The level of GSH was measured by the method described in the previous section.

Mitochondrial membrane potential collapse (ΔΨm%) measurement

For the determination of mitochondrial membrane potential decline, cationic flourogenic probe Rhodamine 123 was used (25). Cell suspension (0.5 mL) was incubated and centrifuged for 1 min at 1000 rpm. The supernatant was removed and Rhodamine (1.5 µM) incubated for 10 min at 37 °C. Then, fluorescence intensity was determined at Excitation: 490 nm and Emission: 520 nm. The capacity of mitochondria to take up the Rhodamine 123 was calculated as the fluorescence difference between the control and test cells.

Measurement of Caspase-3 Activity

Caspase-3 activity was assessed in glial cells lysate by ‘‘Sigma’s caspase-3 assay kit (CASP-3-C)’’ (26). This method is based on the hydrolysis of a peptide substrate (AC-DEVD-pNA) by caspase-3 that leads to release the para-nitro aniline (pNA) moiety. The concentration of pNA released from the substrate was determined by absorption at 405 nm (27).

Assessment of lysosomal membrane stability

Lysosomal membrane stability was measured using acridine orange dye (28). In this method, 1 ml of cell suspension was mixed with 2 mL acridine orange (5 µg/mL) and incubated for 10 min at 37 °C. Then, the fluorescence intensity from distribution of acridine orange to the cytosol was determined at wavelength Excitation: 495 nm: and Emission: 530 nm.

Determination of proteolysis

Proteolysis was measured by fluorescence intensity from tyrosine released into the extracellular space (29). Each of the samples was added trichloroacetic acid (20%) and incubated for 12 h at 4 °C, then, centrifuged (13250 rpm, 10 min). 1-Nitroso-2-naphthol (1 mL) and 1 mL of nitrite acid (10 mg/mL $NaNo_2$ in HNO_3 20%) were added to the supernatant and incubated for 30 min at 37 °C. After the addition of ethylene chloride, the suspension was shaken strongly, and again centrifuged (13250 rpm, 10 min). The fluorescence intensity was measured at Excitation: 460 nm and Emission: 570 nm. The amount of tyrosine was calculated by tyrosine calibration curve (0-100 µM).

Statistical analysis

The homogeneity of variances was tested using Levene’s test. Results were expressed as mean ± SD. All data were statistically analyzed by two-way ANOVA followed by Bonferroni *post hoc* test using GraphPad Prism 8.0. The results with level of significance ($P < 0.05$) were regarded as significant.

Results

Effects of neuropathic pain on the markers of oxidative stress

ROS formation in the glial cells of pain group was significantly higher than the sham group after 6, 10, and 14 days ($P < 0.0001$), but there was not any significant differences between sham and control groups after induction of neuropathic pain (Figure 1). Bonferroni *post hoc* test also indicated that ROS generation in the glial cells of pain group was time-dependent ($P < 0.0001$).

Figures 2 and 3 present the concentration of

reduced and oxidized glutathione, respectively inside and outside the glial cells, at various days after induction of neuropathic pain. The level of intracellular GSH in the pain group on the 2nd and 6th days was considerably higher in contrast the sham group ($P < 0.0001$). On the other hand, GSH in the pain group on the 10th and 14th days were statically lower as compared to the sham group (Figure 2). Besides, two-way ANOVA analysis showed that GSH concentration changes in the glial cells of pain group were time-dependent ($P < 0.0001$).

As presented in Figure 3, on the 2nd, 6th, 10th and 14th days after induction of neuropathic pain, the levels of extracellular GSSG significantly raised in the glial cells of pain group in comparison with sham groups ($P < 0.0001$). In addition, Bonferroni *post hoc* test confirmed that GSSG concentration changes in the glial cells of pain group were time-dependent ($P < 0.0001$).

On the 14th day of pain induction, the levels of GSH in the glial cells of rat neuropathic pain model that incubated with methionine and betaine, the precursors of GSH, were significantly higher than those of the precursors-free pain group (Table 1). The evaluation of glutathione compensatory biosynthesis after incubation of glial cells with methionine and

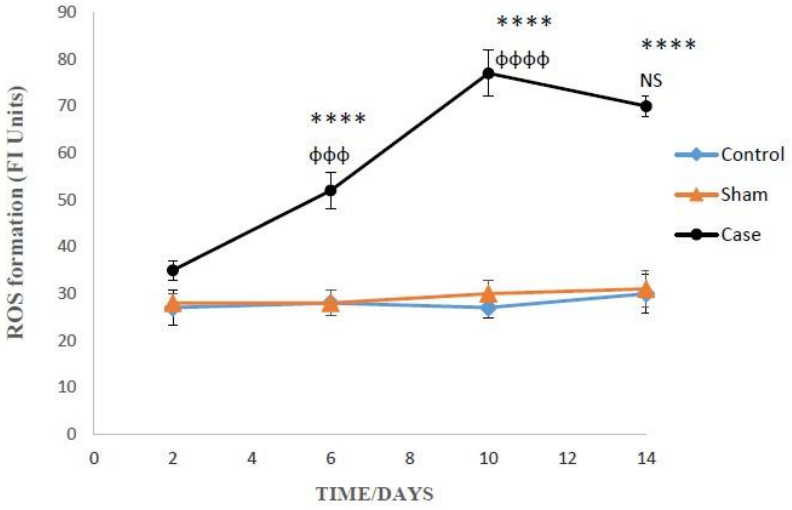

Figure 1. The amounts of ROS production in the glial cells after the induction of neuropathic pain. ROS formation was expressed as fluorescent intensity (FI) units. Values are presented as mean ± SD. $^{****}P < 0.0001$ Significant difference between case and sham groups in corresponding time; $^{\phi\phi\phi}P < 0.001$, $^{\phi\phi\phi\phi}P < 0.0001$ Compared with previous time in case group; NS: Not Significant.

Table 1. Effects of GSH precursors on intracellular GSH in the glial cells on the 14th day after the induction of neuropathic pain.

Groups	Intracellular GSH (µM)			
	Incubation time			
	2 (min)	60 (min)	120 (min)	180 (min)
Control	67 ± 3	64 ± 4	62 ± 4	60 ± 2
Sham	68 ± 3	58 ± 3	54 ± 4	$50 \pm 2^{\#\#\#}$
Case	$22 \pm 2^{****}$	$15 \pm 2^{****}$	$11 \pm 3^{****}$	$6 \pm 2^{****}$
+ Methionine (1 mM)	22 ± 1	$32 \pm 2^{\Phi\Phi\Phi\Phi}$	$43 \pm {}^{1\Phi\Phi\Phi\Phi}$	$41 \pm 2^{\Phi}$
+ Betain (2 mM)	22 ± 2	$36 \pm 1^{\Phi\Phi\Phi\Phi}$	$43 \pm 2^{\Phi\Phi\Phi\Phi}$	$43 \pm 3^{\Phi}$

The glial cells were isolated on the 14th day after the induction of neuropathic pain and their intracellular GSH levels were measured during the time. The values are presented as mean ± SD. $^{\#\#\#}P < 0.001$ Significant difference between sham and control groups in corresponding time; $^{****}P < 0.0001$ Significant difference between case and sham groups in corresponding time; $^{\Phi}P < 0.05$, $^{\Phi\Phi\Phi\Phi}P < 0.0001$ Significant difference between the precursors and case groups in corresponding time.

betaine implies that the biosynthesis pathway of glutathione is functionally active. Besides, the concentrations of intracellular GSH and extracellular GSSG in the sham and control groups did not show significant alterations in different time points after the induction of neuropathic pain (Figures 2 and 3).

Effects of neuropathic pain on mitochondrial membrane potential collapse

Induction of neuropathic pain caused a significant decline of mitochondrial membrane potential (ΔΨm%) in the glial cells in different time points ($P < 0.0001$). ΔΨm% in the sham group was significantly higher than control rats at 6, 10, and 14 days after the pain induction (Figure 4). Moreover, two-way ANOVA analysis showed that ΔΨm% in the glial cells of pain group was time-dependent ($P < 0.0001$) as well as in the glial cells of sham group ($P < 0.05$).

Effects of neuropathic pain on caspase-3 activation

Two-way ANOVA analysis showed significant influence of neuropathic pain on the caspase-3 activity in the glial cells ($P < 0.0001$). However, there was not any significant differences between sham and control groups in caspase-3 activity (Figure 5). Bonferroni *post hoc* tests also indicated that caspase-3 activity in the glial cells of pain group was time-dependent ($P < 0.0001$).

Effects of neuropathic pain on lysosomal membrane leakiness

The lysosomal membrane instability in the glial cells of pain groups was significantly elevated in comparison with the sham group in different time points, while the damage was considerably higher in the glial cells of sham group compared to those of control group at 10 and 14 days after the pain induction ($P < 0.0001$) (Figure 6). Again, Bonferroni *post hoc* test indicated that neuropathic pain had time-dependent effect on lysosomal membrane leakiness ($P < 0.0001$).

Effects of neuropathic pain on cellular proteolysis

Finally, the induction of neuropathic pain leads to the release of tyrosine into the extracellular medium of the glial cells ($P < 0.0001$). Moreover, the cellular proteolysis in the glial cells of the sham group was significantly developed compared to the control group at 10 and 14 days after the pain induction ($P < 0.0001$) (Figure 7). Additionally, two-way ANOVA analysis indicated that neuropathic pain had time dependent effect on cellular proteolysis ($P < 0.0001$).

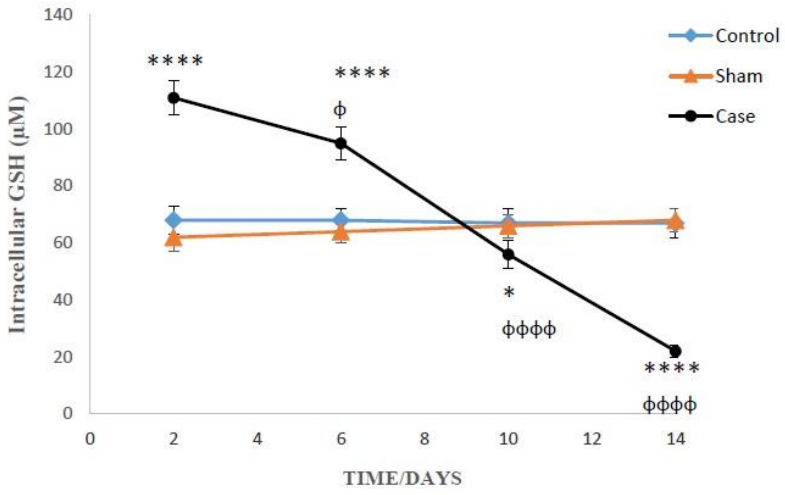

Figure 2. The levels of intracellular GSH the glial cells after the induction of neuropathic pain. Values are presented as mean ± SD. $^{*}P < 0.05$, $^{****}P < 0.0001$ Significant difference between case and sham groups in corresponding time; $^{\phi}P < 0.05$, $^{\phi\phi\phi\phi}P < 0.0001$ Compared with previous time in case group.

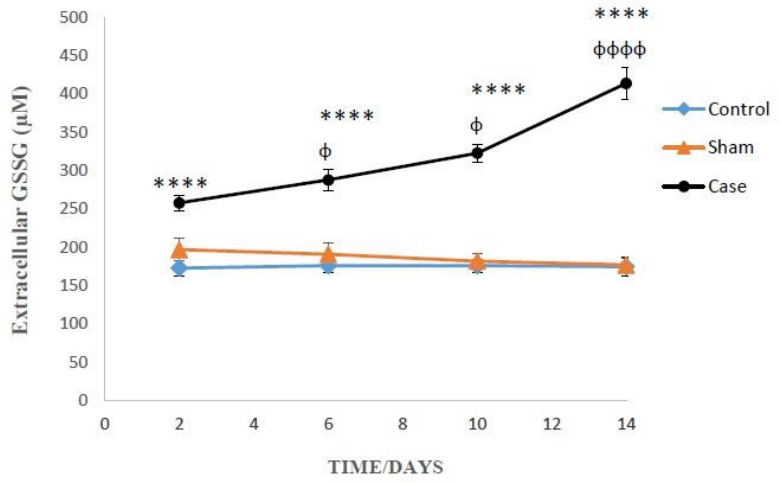

Figure 3. The levels of extracellular GSSG in the glial cells after the induction of neuropathic pain. Values are presented as mean ± SD. $^{****}P < 0.0001$ Significant difference between case and sham groups in corresponding time; $^{\phi}P < 0.05$, $^{\phi\phi\phi\phi}P < 0.0001$ Compared with previous time in case group.

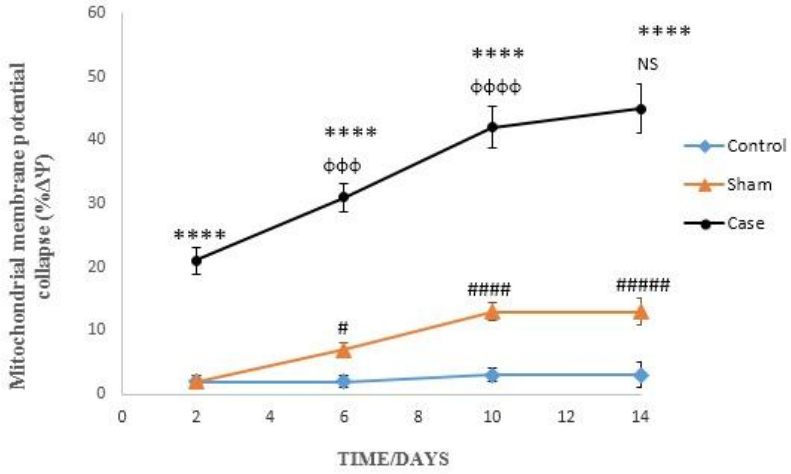

Figure 4. Mitochondrial membrane potential collapse (ΔΨm%) in the glial cells after the induction of neuropathic pain. Values are presented as mean ± SD. $^{****}P < 0.0001$ Significant difference between case and sham groups in corresponding time; $^{\phi\phi\phi}P < 0.001$, $^{\phi\phi\phi\phi}P < 0.0001$ Compared with previous time in case group; NS: Not Significant; $^{\#}P < 0.05$, $^{\#\#\#\#\#}P < 0.0001$ Significant difference between sham and control groups in corresponding time.

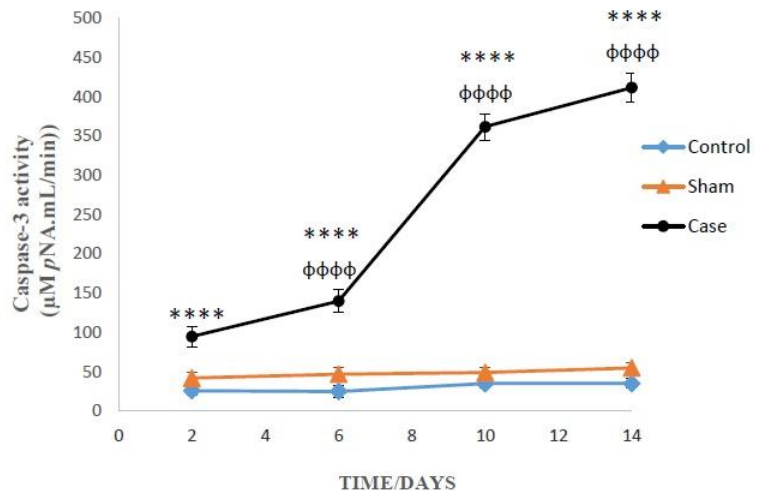

Figure 5. Caspase-3 activity in the glial cells after the induction of neuropathic pain. Values are presented as mean ± SD. $^{****}P < 0.0001$ Significant difference between case and sham groups in corresponding time; $^{\phi\phi\phi\phi}P < 0.0001$ Compared with previous time in case group.

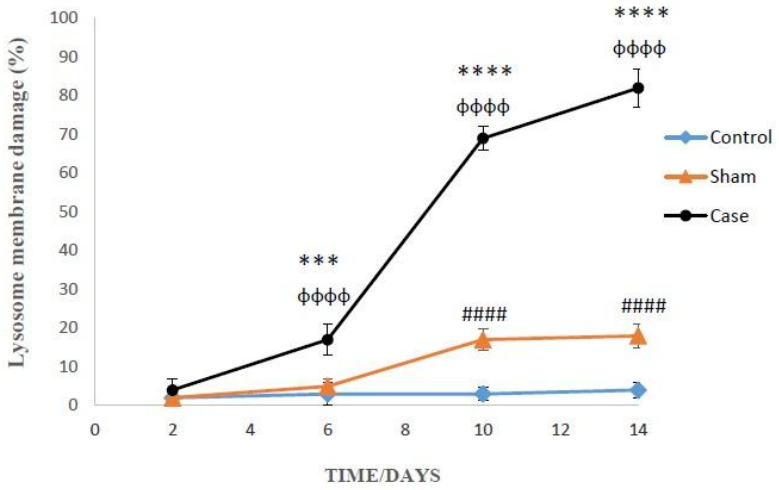

Figure 6. Lysosomal membrane leakiness in the glial cells after the induction of neuropathic pain. Values are presented as mean ± SD. $^{***}P < 0.001$, $^{****}P < 0.0001$ Significant difference between case and sham groups in corresponding time; $^{\phi\phi\phi\phi}P < 0.0001$ Compared with previous time in case group; $^{\#\#\#\#}P < 0.0001$ Significant difference between sham and control groups in corresponding time.

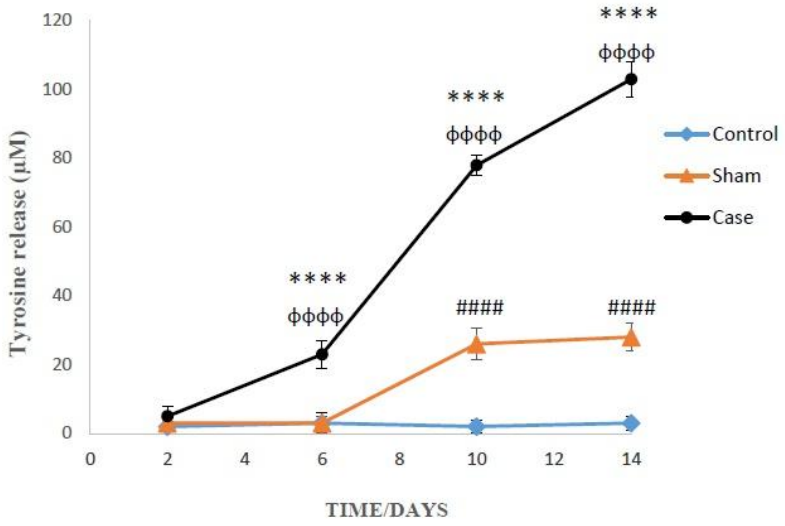

Figure 7. Comparison of cellular proteolysis in the glial cells after the induction of neuropathic pain. Values are presented as mean ± SD. $^{****}P < 0.0001$ Significant difference between case and sham groups in corresponding time; $^{\phi\phi\phi\phi}P < 0.0001$ Compared with previous time in case group; $^{\#\#\#\#}P < 0.0001$ Significant difference between sham and control groups in corresponding time.

Discussion

Glial cells include oligodendrocytes, astrocytes, ependymal cells, and microglia are activated during the formation and maintaining of persistent pain induced by either inflammation or the damage to the peripheral tissues and nerves. Upon activation, glial cells release pro-inflammatory mediators, including ROS, nitric oxide, arachidonic acid, leukotrienes, prostaglandins, and cytokines (12). These stimulators can intensify the pain sensation, and it seems that the brain is more sensitive to oxidative stress than other organs (30). Glial cells release proinflammatory cytokines during neuropathic pain that results in the production of ROS more possible from mitochondria. The generated ROS from the affected areas of the brain can consequently target and damage proteins, DNA, lipids, and cellular organelles. Our results indicated that intracellular ROS formation was increased in the glial cells of the rat brain and ROS production reached its highest level in 14 days after the induction of pain.

GSH and the related enzymatic systems belong to the antioxidant defense system protecting the intracellular biomolecules from oxidative damage (31). Inactivation of ROS causes the oxidation of GSH into GSSG that can either be recycled to GSH or removed from the intracellular milieu through specialized transporters. In the present study, the levels of intracellular GSH considerably increased at 2 and 6 days after the pain induction, which could be due to GSH rapid synthesis in response to oxidative stress (32). However, the levels of GSH were rigorously diminished on the 10th and 14th day of pain induction that may be due to severe ROS detoxification in this group. Rapid GSSG formation along with the inadequate levels of GSH indicate the unbalanced redox states and the incidence of oxidative stress, a condition that may lead to cell death. In addition, in this study the role of methionine and betaine as precursors of biosynthesis for GSH was investigated. The obtained results indicated that methionine and betaine as the precursors of GSH biosynthesis triggered GSH synthesis in the affected glial cells yet again. Therefore, the level of GSH in this group was significantly higher than 14th day pain group. Obviously, the reduction of intracellular GSH in pain groups might be solely due to neuropathic pain-induced oxidative stress.

The reduction of mitochondrial membrane potential is an important indicator for assessing the mitochondrial damage. Thiol oxidation in the mitochondrial membrane by ROS and MPT pore opening have been recurrently used for diagnosis of mitochondrial dysfunction and subsequent cellular events (33). The reduction of mitochondrial membrane potential by MPT pore opening would permeabilize mitochondrial membrane that leads to cellular damage and the initiation of apoptosis. As shown in Figure 4, decline in mitochondrial membrane potential as a marker of mitochondrial damage was increased on the second day of pain induction. It is suggested that the oxidative stress ensued upon the neuropathic pain induction would proceed to the mitochondrial dysfunction. It seems that over the time, the damage to mitochondria going to be more severe and in fourteenth day it was at the highest level.

Our results indicated that caspase-3 activity in the pain group was dramatically increased, which may be due to the cascade of events begin from huge ROS formation after induction of persistent pain. These toxic events eventually proceed to the opening of MPT pore and subsequent releasing of cytochrome C. The release of cytochrome c from mitochondria into cytosol following the MPT pore opening is a key initiating step in both apoptotic and necrotic cell death processes in intact cells (34).

In this study, the effect of neuropathic pain stress on lysosomes was also studied. In recent years, it has been found that partial and selective permeability of lysosomes was followed by the release of proteolytic enzymes especially cathepsins (B, D, L) Apparently, hydroxyl radicals formed through the Haber-Weiss reaction inside the lysosomes (catalyzed by iron), provoke the lysosome membrane damage. Leakage of lysosomal enzymes would increase H_2O_2 production in mitochondria and finally lead to further lysosomal permeabilization, since H_2O_2 released from mitochondria can easily penetrate into the lysosomes and start the Haber-Weiss reaction again (35). Our results confirmed such cascades of events and show that neuropathic pain could increase lysosomal membrane fragility and leakiness as a consequence of ROS generation that directly contribute to cell death. Lysosomal membrane damage caused cellular proteolysis that was determined by measuring the extracellular tyrosine. It can be said that by promotion of pain duration and intensity, lysosomal leakage and proteolysis occurred in the glial cells of rat brain that ultimately end to cellular death.

In conclusion, our results confirmed that neuropathic pain has different toxic effects in the rat brain glial cells, including elevated ROS generation, GSH depletion, mitochondrial dysfunction, activation of caspases cascade, lysosomal membrane leakiness, and cellular proteolysis. Our findings contribute to a better understanding of toxic mechanisms of neuropathic pain in the glial cells of rat brain.

Acknowledgments

The results presented in this paper were partly from thesis of Dr. Lida Karimian Pharm.D. graduate of School of Pharmacy, Shahid Beheshti University of Medical Sciences, who performed her thesis under supervision of Professor Jalal Pourahmad and late Professor Bizhan Shafaghi. The investigation was carried out at Dept. of Toxicology, School of Pharmacy, Shahid Beheshti University of Medical Sciences, Tehran, Iran.

References

(1) Brodal P. A neurobiologist's attempt to understand persistent pain. *Scand. J. Pain.* (2017) 15: 140-7.
(2) Woolf CJ. Pain: moving from symptom control toward mechanism-specific pharmacologic management. *Annal. Int. Med.* (2004) 140: 441-51.
(3) Gunduz A, Eraydin I, Turkmen S, Kalkan OF, Turedi S, Eryigit U and Ayar A. Analgesic effects of mad honey (grayanotoxin) in mice models of acute pain and painful diabetic neuropathy. *Hum. Exp. Toxicol.* (2014) 3: 130-5.
(4) Dunne FJ, Getachew H, Cullenbrooke F and Dunne C. Pain and pain syndromes. *Br. J. Hosp. Med. (Lond)* (2018) 79: 449-53.
(5) Stucky CL, Gold MS and Zhang X. Mechanisms of pain. *Proc. Natl. Acad. Sci. USA.* (2001) 98: 11845-6.
(6) Tsuda M, Inoue K and Salter MW. Neuropathic pain and spinal microglia: a big problem from molecules in "small" glia. *Trends Neurosci.* (2005) 28: 101-7.
(7) Cohen SP and Mao J. Neuropathic pain: mechanisms

and their clinical implications. *BMJ* (2014) 348: f7656.
(8) Watkins LR, Milligan ED and Maier SF. Glial activation: a driving force for pathological pain. *Trends Neurosci.* (2001) 24: 450-5.
(9) Watkins LR, Milligan ED and Maier SF. Spinal cord glia: new players in pain. *Pain* (2001) 93: 201-5.
(10) Woolf CJ. Dissecting out mechanisms responsible for peripheral neuropathic pain: implications for diagnosis and therapy. *Life Sci.* (2004) 74: 2605-10.
(11) Gosselin RD, Suter MR, Ji RR and Decosterd I. Glial cells and chronic pain. *Neuroscientist* (2010) 16: 519-31.
(12) Watkins LR and Maier SF. Glia: a novel drug discovery target for clinical pain. *Nat. Rev. Drug Discov.* (2003) 2: 973-85.
(13) Hashizume H, Rutkowski MD, Weinstein JN and DeLeo JA. Central administration of methotrexate reduces mechanical allodynia in an animal model of radiculopathy/sciatica. *Pain* (2000) 87: 159-69.
(14) Sweitzer SM, Schubert P and DeLeo JA. Propentofylline, a glial modulating agent, exhibits antiallodynic properties in a rat model of neuropathic pain. *J. Pharmacol. Exp. Ther.* (2001) 297: 1210-7.
(15) Watkins LR, Maier SF. The pain of being sick: implications of immune-to-brain communication for understanding pain. *Annu. Rev. Psychol*. (2000) 51: 29-57.
(16) Meller ST, Dykstra C, Grzybycki D, Murphy S and Gebhart GF. The possible role of glia in nociceptive processing and hyperalgesia in the spinal cord of the rat. *Neuropharmacology* (1994) 33: 1471-8.
(17) Milligan ED, Mehmert KK, Hinde JL, Harvey LO, Martin D, Tracey KJ, Maier SF and Watkins LR . Thermal hyperalgesia and mechanical allodynia produced by intrathecal administration of the human immunodeficiency virus-1 (HIV-1) envelope glycoprotein, gp120. *Brain Res.* (2000) 861: 105-16.
(18) Watkins LR, Martin D, Ulrich P, Tracey KJ and Maier SF. Evidence for the involvement of spinal cord glia in subcutaneous formalin induced hyperalgesia in the rat. *Pain* (1997) 71: 225-35.
(19) Whiteside GT and Munglani R. Cell death in the superficial dorsal horn in a model of neuropathic pain. *J. Neurosci Res.* (2001) 64: 168-73.
(20) Li S, Yang C, Fang X, Zhan G, Huang N, Gao J, Xu H, Hashimoto K and Luo A. Role of Keap1-Nrf2 signaling in anhedonia symptoms in a rat model of chronic neuropathic pain: improvement with sulforaphane. *Front Pharmacol.* (2018) 9: 887.
(21) Decosterd I and Woolf CJ. Spared nerve injury: an animal model of persistent peripheral neuropathic pain. *Pain* (2000) 87: 149-58.
(22) Frank MG, Wieseler-Frank JL, Watkins LR and Maier SF. Rapid isolation of highly enriched and quiescent microglia from adult rat hippocampus: Immunophenotypic and functional characteristics. *J. Neurosci. Methods* (2006) 151: 121-30.
(23) Pourahmad J and O'Brien PJ. Biological reactive intermediates that mediate chromium (VI) toxicity. *Adv. Exp. Med. Biol.* (2001) 500: 203-7.
(24) Hissin PJ and Hilf R. A fluorometric method for determination of oxidized and reduced glutathione in tissues. *Anal. Biochem.* (1976) 74: 214-26.
(25) Faizi M, Salimi A, Seydi E, Naserzadeh P, Kouhnavard M, Rahimi A and Pourahmad J. Toxicity of cuprizone a Cu(2+) chelating agent on isolated mouse brain mitochondria: a justification for demyelination and subsequent behavioral dysfunction. *Toxicol. Mech. Methods* (2016) 26: 276-83.
(26) Nicholson DW, Ali A, Thornberry NA, Vaillancourt JP, Ding CK, Gallant M, Gareau Y, Griffin PR, Labelle M and Lazebnik YA. Identification and inhibition of the ICE/CED-3 protease necessary for mammalian apoptosis. *Nature* (1995) 376: 37-43.
(27) Sakahira H, Enari M and Nagata S. Cleavage of CAD inhibitor in CAD activation and DNA degradation during apoptosis. *Nature* (1998) 391: 96-9.
(28) Pourahmad J, Mortada Y, Eskandari MR and Shahraki J. Involvement of Lysosomal Labilisation and Lysosomal/mitochondrial Cross-Talk in Diclofenac Induced Hepatotoxicity. *Iran. J. Pharm. Res.* (2011) 10: 877-87.
(29) Novak RF, Kharasch ED and Wendel NK. Nitrofurantoin-stimulated proteolysis in human erythrocytes: a novel index of toxic insult by nitroaromatics. *J. Pharmacol. Exp. Ther.* (1988) 247: 439-44.
(30) Kreutzberg GW. Microglia: a sensor for pathological events in the CNS. *Trends Neurosci.* (1996) 19: 312-8.
(31) Gholami S, Hosseini MJ, Jafari L, Omidvar F, Kamalinejad M, Mashayekhi V, Hosseini SH, Kardan A, Pourahmad J and Eskandari MR. Mitochondria as a target for the cardioprotective effects of *Cydonia oblonga* Mill. and *Ficus carica* L. in doxorubicin-induced cardiotoxicity. *Drug Res. (Stuttg)* (2017) 67: 358-65.
(32) Hammond CL, Lee TK and Ballatori N. Novel roles for glutathione in gene expression, cell death, and membrane transport of organic solutes. *J. Hepatol.* (2001) 34: 946-54.
(33) Pourahmad J and Hosseini MJ. Application of isolated mitochondria in toxicological and clinical studies. *Iran. J. Pharm. Res.* (2012) 11: 703-4.

(34) Gogvadze V, Orrenius S and Zhivotovsky B. Multiple pathways of cytochrome c release from mitochondria in apoptosis. *Biochim. Biophys. Acta* (2006) 1757: 639-47.

(35) Pourahmad J, Eskandari MR, Alavian G and Shaki F. Lysosomal membrane leakiness and metabolic biomethylation play key roles in methyl tertiary butyl ether-induced toxicity and detoxification. *Toxicol. Environ. Chem.* (2012) 94: 281-93.

This article is available online at http://www.ijpr.ir